IOPscience iopscience.iop.org

Home Search Collections Journals About Contact us My IOPscience

Realization of an atomically flat surface of diamond using dressed photon–phonon etching

This article has been downloaded from IOPscience. Please scroll down to see the full text article.

2012 J. Phys. D: Appl. Phys. 45 475302

(http://iopscience.iop.org/0022-3727/45/47/475302)

View the table of contents for this issue, or go to the journal homepage for more

Download details:
IP Address: 133.11.90.145
The article was downloaded on 31/10/2012 at 05:41

Please note that terms and conditions apply.

IOP PUBLISHING JOURNAL OF PHYSICS D: APPLIED PHYSICS

J. Phys. D: Appl. Phys. **45** (2012) 475302 (4pp) doi:10.1088/0022-3727/45/47/475302

Realization of an atomically flat surface of diamond using dressed photon–phonon etching

Takashi Yatsui[1,2], Wataru Nomura[1], Makoto Naruse[3] and Motoichi Ohtsu[1]

[1] School of Engineering, University of Tokyo, Bunkyo-ku, Tokyo 113-8656, Japan
[2] Advanced Low Carbon Technology Research and Development Program (ALCA), Japan Science and Technology Agency, Kawaguchi-shi, Saitama 332-0012, Japan
[3] National Institute of Information and Communications Technology, 4-2-1 Nukui-kita, Koganei, Tokyo 184-8795, Japan

E-mail: yatsui@ee.t.u-tokyo.ac.jp

Received 20 August 2012, in final form 4 October 2012
Published 30 October 2012
Online at stacks.iop.org/JPhysD/45/475302

Abstract

We obtained an atomically flat diamond surface following dressed photon–phonon (DPP) etching using 3.81 eV light and O_2 gas. We obtained a surface roughness (R_a) of 0.154 nm for Ib-type (1 1 1) diamond and 0.096 nm for Ib-type (1 0 0) diamond. To evaluate the surface roughness, we grouped the surface into bins of width l and introduced the standard deviation of the height difference function for a given separation l, which allowed us to determine the height variation of the surface. Based on the calculation of standard deviation, the conventional adiabatic photochemical reaction did not remove the small surface features, while DPP etching decreased the surface roughness for all length scales.

(Some figures may appear in colour only in the online journal)

Realization of ultra-flat diamond substrate surfaces is required for a variety of future applications, including light-emitting devices [1], power devices [2] and quantum communication [3]. Although mechanical polishing has been used to flatten the surfaces, there are difficulties due to the hardness of diamond. We have developed a non-contact self-organized near-field etching [4] capable of producing atomically flat diamond.

The optical near-field is a virtual photon coupled with an excited electron. The quasiparticle representing this coupled state has been called a dressed photon (DP) with a greater amount of energy than a free photon due to the contribution from the energy of the coupled electron. The DP has been theoretically described by assuming a multipolar quantum electrodynamic Hamiltonian in a Coulomb gauge and single-particle states in a finite nano-system [5]. After a unitary transformation and some simple calculations, the creation and annihilation operators of the DP are expressed as the sum of the operators of the free photon and an electron–hole pair. The DP also interacts with the crystal lattice structure of nanomaterials by coupling with the multimodes of the phonons. As a result, the DP can couple with the phonons in a coherent state [6], and the combined coupled state of DP and coherent phonon quasiparticle, referred to as a dressed photon and phonon (DPP), has a higher energy than the DP or the incident free photon. Numerous experiments have been reported, in which the results were explained by DPP theory, including photochemical vapour deposition [7], photolithography [8], visible-light water splitting [9], photovoltaic devices [10] and energy up-conversion devices [11]. Based on these theoretical studies and experiments, we succeeded in realizing an Ångström-scale flattened glass substrate [4]. Here, we apply this method to a diamond substrate.

When non-focused propagating light is irradiated on the substrate, a DPP is generated at the protrusions of the substrate (figure 1(*a*)). If the dissociation energy, E_d, of the etching gas is higher than the photon energy, E, of the propagating light, the conventional adiabatic photochemical reaction of the gas is avoided. However, due to the higher energy of the DPP, the etching gas is selectively dissociated at the protrusions on the surface (figure 1(*b*)). The dissociated etching gas

 © 2012 IOP Publishing Ltd Printed in the UK & the USA

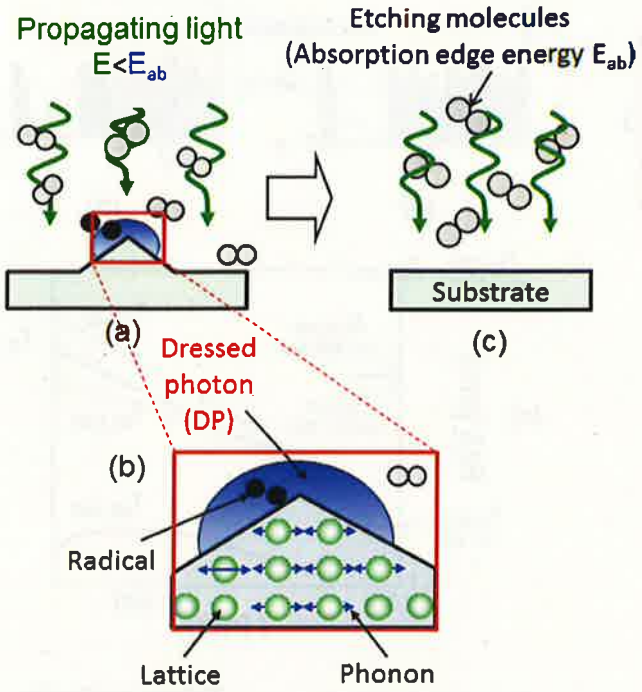

Figure 1. Schematic of DPP etching. (*a*) Etching gas (absorption edge energy E_{ab}) is selectively photodissociated at the protrusions and the activated etching gas atoms etch away the protrusions. (*b*) Magnified schematic of (*a*). (*c*) DPP etching automatically stops when the substrate becomes sufficiently flat.

then etches away the surface features, and the etching process automatically stops when the surface becomes flat (figure 1(*c*)).

We used O_2 gas to perform DPP etching on a diamond substrate, which has a dissociation energy of 5.12 eV (E_d) [12]. A continuum wave He–Cd laser with a wavelength of 325 nm (3.81 eV) and an excitation power of 0.8 W cm^{-2} was used to dissociate the O_2 gas through a DPP reaction, inducing the oxygen radical O* to produce an ultra-flat surface. This photon energy is lower than E_d, so that the conventional O_2 adiabatic photochemical reaction is avoided. Note that a laser power density of the order of W cm^{-2} is 10^{15} times smaller than that of multiple photon processing using an ultra-short pulse laser [13]. Therefore, the DPP etching process did not originate from a conventional multiple photon excitation process [14].

We used a single-crystalline diamond substrate grown under high pressure and high temperature [15]. We performed the DPP etching under atmosphere conditions using a Ib-type (absorption band edge of 3.02 eV) diamond (1 1 1) substrate prepared by cleaving. The surface roughness, R_a, was evaluated using an atomic force microscope (AFM), in which all images were obtained using tapping mode and a cantilever with a 15 nm tip diameter. Figures 2(*a*)–(*c*) show typical AFM images with a 10 μm × 10 μm of scanning area before DPP etching, after 30 min of etching and after 60 min of etching, respectively. The scanned area was 256 × 256 pixels with a spatial resolution of 40 nm. The R_a value before etching was 0.660 nm (figure 2(*a*)), comparable to the reported value of the ultra-flat substrate [16]. We confirmed that the standard deviation of R_a for figure 2(*a*) was small (0.0022) through 20 times repeated measurements.

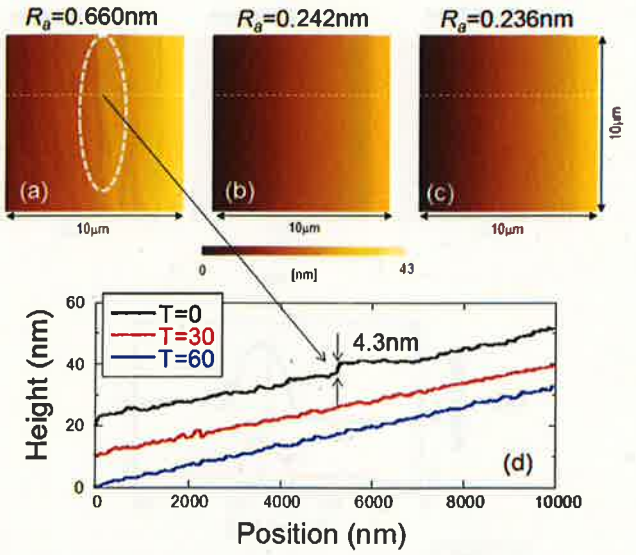

Figure 2. Typical AFM images of the Ib-type diamond (1 1 1) substrate with a 10 μm × 10 μm scanning area. Etching time T: (*a*) 0 min (before etching), (*b*) 30 min and (*c*) 60 min with a surface roughness R_a of (*a*) 0.660 nm, (*b*) 0.242 nm and (*c*) 0.236 nm, respectively. (*d*) Cross-sectional profile along the white dashed lines in (*a*)–(*c*).

Hence, we considered that the change in the R_a value due to the change in the shape of the cantilever apex could be excluded. By comparing figures 2(*a*)–(*c*), we found that the R_a value decreased to 0.236 nm after 60 min of DPP etching. The cross-sectional profiles along the white dashed lines in figures 2(*a*)–(*c*) show that a large step (4.3 nm) was observed in figure 2(*a*) (before DPP etching); however, as shown inside the dashed white ellipse, flat surfaces without a large step were obtained after DPP etching (figures 2(*b*) and (*c*)). We also obtained AFM images with a 5 μm × 5 μm scanning area. Figures 3(*a*), (*b*) and (*c*) correspond to figures 2(*a*), (*b*) and (*c*), respectively. The scanned area was 256 × 256 pixels with a spatial resolution of 20 nm, which was comparable to the tip diameter of the cantilever. These smaller scanning area images were confirmed to have similar R_a decreases (from 0.457 to 0.154 nm). In addition, we compared the cross-sectional profile of the bump indicated as A–A′ in figure 3(*a*) and C–C′ in figure 3(*c*) (see figure 3(*d*)). This revealed a drastic reduction in height (from 11.32 to 5.82 nm) and a full-width at half-maximum (FWHM) from 103 to 83 nm. These results support the DPP etching and show flattening of the surface, as described above.

Figure 3(*e*) shows the cross-sectional profiles of figures 3(*a*)–(*c*), showing the decrease in the surface roughness. Additionally, 60 min DPP etching resulted in an ultra-flat surface with atomic steps. Based on the (1 1 1) crystal plane of the substrate, we calculated the size of each step in units of the lattice spaces, a, as 0.206 nm. The dashed horizontal lines in figure 3(*f*) show the average height of each terrace. The average heights were not exactly the same but close to integer multiples of a, because the height was an average value along each step as long as 200 nm, indicating that the observed flat terraces were atomic steps of the diamond (1 1 1) plane.

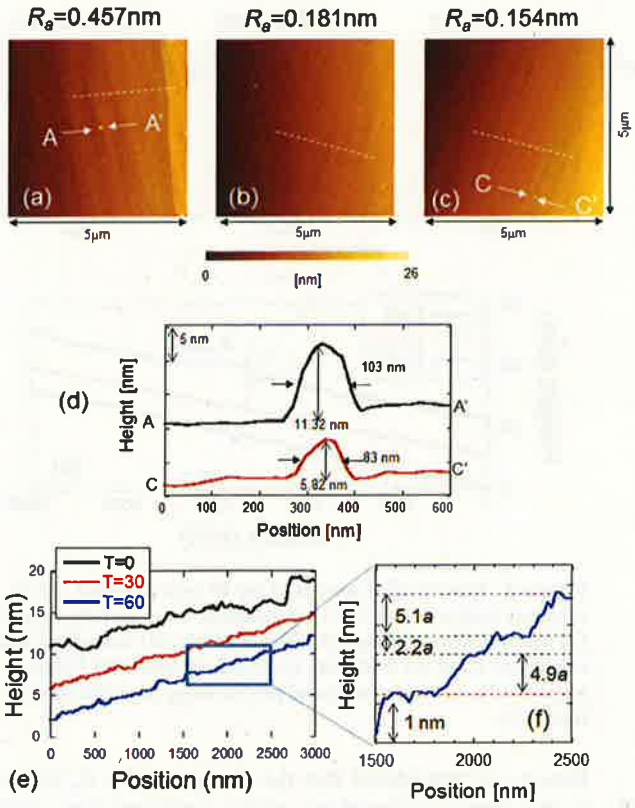

Figure 3. Typical AFM images of the Ib-type diamond (1 1 1) substrate with 5 μm × 5 μm scanning area. Etching time T: (*a*) 0 min (before etching), (*b*) 30 min and (*c*) 60 min with a surface roughness, R_a, of (*a*) 0.457 nm, (*b*) 0.181 nm and (*c*) 0.154 nm, respectively. (*d*) Cross-sectional profile along A–A′ in figure (*a*) and C–C′ in (*c*). (*e*) Cross-sectional profiles of (*a*)–(*c*). (*f*) Magnified profile of (*e*).

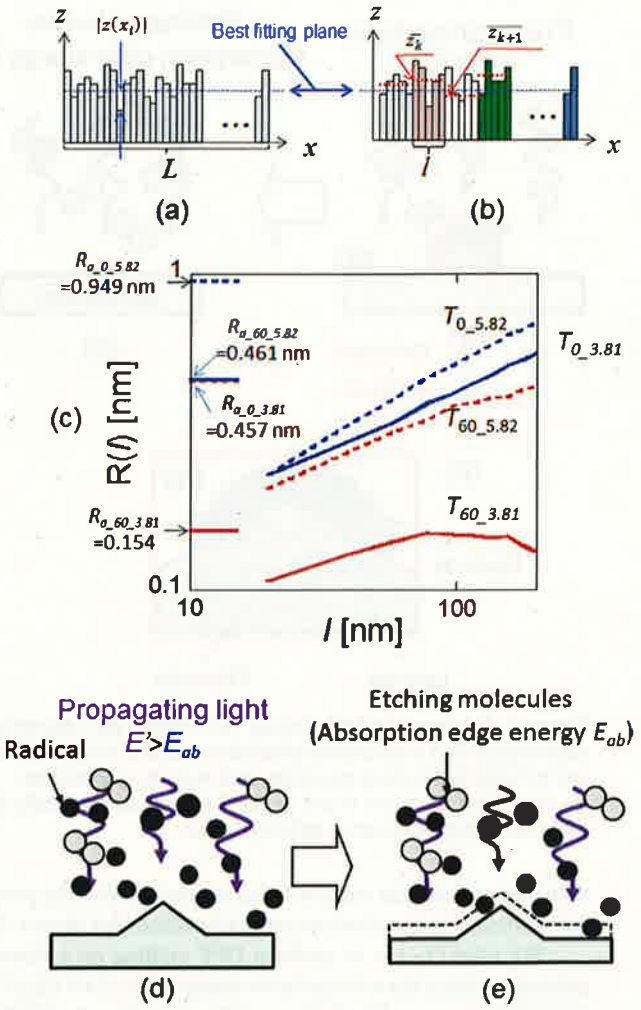

Figure 4. Schematic of (*a*) surface roughness R_a and (*b*) standard deviation $R(l)$. (*c*) Calculated values of $R(l)$. T_{0_325} (0 min), T_{30} (30 min) and T_{60} (60 min). (*d*), (*e*) Schematic of the conventional adiabatic photochemical etching.

The parameter R_a is an arithmetic average of the absolute values of the surface height deviations measured from the best-fitting plane (as shown in the blue dashed line in figures 4(*a*) and (*b*)), which was used to produce AMF images with tilt compensation using the third-order least-squares method. The R_a value is given by

$$R_a = \frac{1}{L}\int_0^L |z(x)|\mathrm{d}x \cong \frac{1}{n}\sum_{i=1}^{n} |z(x_i)|,$$

where $|z(x_i)|$ are the absolute values measured from the best-fitting plane and L is the evaluation length. Physically, dx corresponds to the spatial resolution in the measurement of $f(x)$ and n is the number of pixels in the measurement; $n = L/\mathrm{d}x$. This gives information about the surface roughness, but it is the average value of the roughness for an entire region. Consequently, we calculated the standard deviation of the height difference function $R(l)$ $(=\sqrt{\langle(\overline{z_{k+1}} - \overline{z_k})^2/2\rangle})$, figure 4(*b*)) [17], where l is the bin size and separation, z is the height and $\overline{z_k}$ is the average z value of the bin. Using $R(l)$, we found contributions of different length scales to the overall surface roughness. The scanned area of all images was 256 × 256 pixels with a spatial resolution of 20 nm.

Curves $T_{0\_3.81}$ and $T_{60\_3.81}$ in figure 4(*c*) represent the $R(l)$ at etching times of 0 and 60 min, respectively. These results indicated that the value of $R(l)$ decreased for all values of l. The order of magnitude of the $R(l)$ values was comparable to the R_a values, and $R(l)$ decreased as the R_a value decreased. We also performed conventional photochemical etching using 5.82 eV light (λ = 213 nm, 20 Hz, pulse width = 5 ns), with a photon energy higher than E_d of 5.12 eV. This induced an adiabatic photochemical reaction in the gas. Etching for 60 min with 5.82 eV light resulted in a drastic decrease in the surface roughness from 0.949 nm (R_a_0_5.82) to 0.461 nm (R_a_60_5.82). However, by comparing the $R(l)$ curves for 5.82 eV etch, $T_{0\_5.82}$ (0 min) and $T_{60\_5.82}$ (60 min) in figure 4(*c*), we found that $R(l)$ remained unchanged for l = 20 nm. Because the tip of the protrusion on the substrate had a larger surface area and a higher etching rate, we expected a reduction in surface roughness. However, 5.82 eV light induced the adiabatic photochemical reaction of the gas (figure 4(*d*)), which did not selectively etch the protrusions. Thus, etching with 5.82 eV light did not change the profiles of the nano-scale surface roughness (figure 4(*e*)).

We performed DPP etching using IIa-type (absorption band edge of below 5.50 eV [18]) diamond (1 1 1) with a

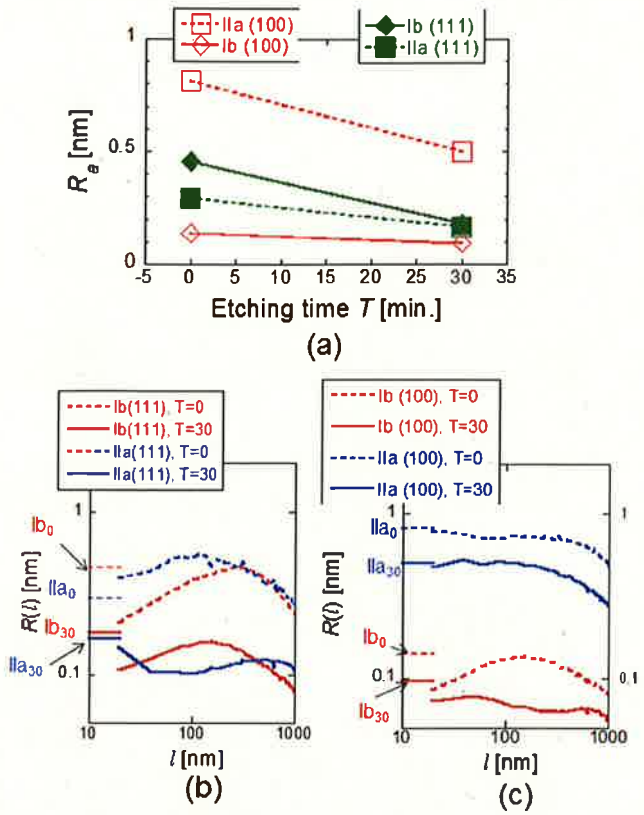

Figure 5. (*a*) Dependence of R_a values on the etching time T with 3.81 eV light. (*b*) Calculated values of $R(l)$ for the (1 1 1) substrate. (*c*) Calculated values of $R(l)$ for the (1 0 0) substrate.

continuum wave He–Cd laser with a wavelength of 325 nm (3.81 eV) and an excitation power of 0.8 W cm^{-2}. Figure 5(*a*) shows the decrease in R_a from 0.294 to 0.166 nm. In addition, DPP etching was performed on a diamond (1 0 0) substrate. The (1 0 0) substrate was also grown under high-pressure and high-temperature conditions. The (1 0 0) substrate was mechanically polished by a conventional method before DPP etching, so that it had a flat surface with R_a less than 1.0 nm. This value was comparable to the ultra-flat surface prepared by ion implantation after mechanical polishing [19]. Using those (1 0 0) substrates, we found the decrease in the R_a value after a 30 min DPP etch (see figure 5(*a*)). Although the initial R_a for IIa-type (1 0 0) was as high as 0.813 nm, the rate of decrease in the R_a value for IIa-type (1 0 0) (10.4×10^{-3} nm min^{-1}, open squares in figure 5(*a*)) was comparable to the rate for Ib-type (1 1 1) (9.2×10^{-3} nm min^{-1}, solid diamonds in figure 5(*a*)). The minimum R_a value of 0.096 nm was obtained for Ib-type (1 0 0) following a 30 min DPP etching. Figures 5(*b*) and (*c*) show the calculated $R(l)$ values, indicating that the DPP etch decreased $R(l)$ for all value of l.

In conclusion, we performed DPP etching on a diamond substrate. Using 3.81 eV light and O_2 gas, we obtained an atomically flat surface with a surface roughness R_a of 0.154 nm (Ib-type (1 1 1)) and 0.096 nm (Ib-type (1 0 0)). By introducing the standard deviation, $R(l)$, we found that the conventional adiabatic photochemical reaction did not remove the smallest surface features, while DPP etching decreased the surface roughness for all length scales. Because DPP etching is a non-contact method and does not cause damage due to polishing, it will improve the electrical and optical performance in a variety of applications. DPP etching can be applied not only to flat but also to three-dimensional surfaces including convex, concave and periodic profiles [20].

References

[1] Makino T, Tokuda N, Kato H, Kanno S, Yamasaki S and Okushi H 2008 *Phys. Status Solidi* a **205** 2200
[2] Denisenko A and Kohn E 2005 *Diamond Relat. Mater.* **14** 491
[3] Gruber A, Dräbenstedt A, Tietz C, Fleury L, Wrachtrup J and von Borczyskowski C 1997 *Science* **276** 2012
[4] Yatsui T, Hirata K, Nomura W, Tabata Y and Ohtsu M 2008 *Appl. Phys.* B **93** 55
[5] Kobayashi K, Sangu S, Ito H and Ohtsu M 2000 *Phys. Rev.* A **63** 013806
[6] Sato A, Tanaka Y, Minami F and Kobayashi K 2009 *J. Lumin.* **129** 1718
[7] Kawazoe T, Kobayashi K, Takubo S and Ohtsu M 2005 *J. Chem. Phys.* **122** 024715
[8] Yonemitsu H, Kawazoe T, Kobayashi K and Ohtsu M 2007 *J. Lumin.* **122–123** 230
[9] Le T H H, Mawatari K, Pihosh Y, Kawazoe T, Yatsui T, Ohtsu M, Tosa M and Kitamori T 2011 *Appl. Phys. Lett.* **99** 213105
[10] Yukutake S, Kawazoe T, Yatsui T, Nomura W, Kitamura K and Ohtsu M 2010 *Appl. Phys.* B **99** 415
[11] Kawazoe T, Fujiwara H, Kobayashi K and Ohtsu M 2009 *IEEE J. Sel. Top. Quantum Electron.* **15** 1380
[12] Keilin D and Hartree E F 1950 *Nature* **165** 543
[13] Miyaji G and Miyazaki K 2008 *Opt. Exp.* **16** 16265
[14] Kawata S, Sun H-B, Tanaka T and Takada K 2001 *Nature* **412** 697
[15] Sumiya H, Toda N and Satoh S 2002 *J. Cryst. Growth* **237–239** 1281
[16] Tokuda N, Umezawa H, Kato H, Ogura M, Gonda S, Yamabe K, Okushi H and Yamasaki S 2009 *Appl. Phys. Express* **2** 055001
[17] Allan D W 1966 *Proc. IEEE* **54** 221
[18] Clark C, Dean P and Harris P 1964 *Proc. R. Soc. Lond.* A **277** 312
[19] Tran Thi T N, Fernandez B, Eon D, Gheeraert E, Härtwig J, Lafford T, Perrat-Mabilon A, Peaucelle C, Olivero P and Bustarret E 2011 *Phys. Status Solidi* a **208** 2057
[20] Yatsui T, Hirata K, Tabata Y, Miyake Y, Akita Y, Yoshimoto M, Nomura W, Kawazoe T, Naruse M and Ohtsu M 2011 *Appl. Phys.* B **103** 527